PROCEEDINGS OF SCIENCE

ONLINE ICRC 2021
THE ASTROPARTICLE PHYSICS CONFERENCE
Berlin | Germany
37th International Cosmic Ray Conference
12–23 July 2021

νSpaceSim: A Comprehensive Simulation for the Modeling of Optical and Radio Signals from Extensive Air Showers Induced by Cosmic Neutrinos for Space-based Experiments

John F Krizmanic[a,b,c,*] **on behalf of the νSpaceSim Collaboration**
(a complete list of authors can be found at the end of the proceedings)

[a] *University of Maryland, Baltimore County, Center for Space Sciences and Technology*
1000 Hilltop Cir, Baltimore, Maryland 21250 USA
[b] *Center for Research and Exploration in Space Science & Technology*
[c] *NASA/Goddard Space Flight Center, Code 661*
8800 Greenbelt Rd, Greenbelt, Maryland 20771 USA
E-mail: john.f.krizmanic@nasa.gov

νSpaceSim is a comprehensive end-to-end simulation package to model the optical and radio signals from extensive air showers (EAS) induced by cosmic neutrino interactions. The development has initially focused on modeling the upward-moving EASs sourced from tau neutrino interactions within the Earth that employs a new modeling package, `nuPyProp`. *νSpaceSim* is designed to model all aspects of the processes that lead to the neutrino-induced EAS signals, including the modeling of the neutrino interactions inside the Earth, propagating the leptons into the atmosphere, modeling the tau-lepton decays, forming composite EAS, generating the air optical Cherenkov and radio signals, modeling their propagation through the atmosphere, including using a MERRA-2 database driven application to generate cloud maps, and modeling detector responses. *νSpaceSim* uses a vectorized Python implementation of a sampled library approach to efficiently simulate neutrino-induced and background signals at a specific orbit or balloon altitude. A detector response module, based on user-inputted response parameters, subsequently is used to record the events and determine acceptance. The framework will allow for the calculation of the sky coverage and the pointing requirements needed for target-of-opportunity (ToO) follow-up observations of transients, as well as the assessment of the effects of dark-sky airglow and UHECR backgrounds. *νSpaceSim* will provide an efficient and practical cosmic neutrino EAS signal generation modeling package to aid in the development of future sub-orbital and space-based experiments. In this paper, the *νSpaceSim* framework, physics modeling, and the cosmic neutrino measurement capabilities of the current β-version are discussed with an example experimental configuration are presented as well as a discussion of additional features currently under development.

37th International Cosmic Ray Conference (ICRC 2021)
July 12th – 23rd, 2021
Online – Berlin, Germany

*Presenter

PoS(ICRC2021)1205

1. Introduction

The measurement of the spectra and variability of the Very-High Energy (VHE: $E_\nu \gtrsim 1$ PeV) neutrino component of cosmic radiation and its angular distribution on the sky provide a unique probe of high-energy astrophysical phenomena, especially in a multi-messenger (MM) astrophysics context. The results from IceCube [1, 2] demonstrate the existence of an extra-solar system astrophysical neutrino flux with neutrino energies from > 10 TeV to potentially ~ 10 PeV, including an event consistent with the Glashow resonance at 6.3 PeV [3]. The IceCube observation [4] of a neutrino coincident with gamma-rays from the blazar flare TXS 0506+056 and the association with a neutrino detection with a Tidal Disruption Event [5] demonstrate both the strength of MM astrophysics and the need to detect neutrino transient events. As an example of the potential for space-based neutrino experiments, simulation results for the Probe Of Extreme Multi-Messenger Astrophysics (POEMMA) mission [6] demonstrate significant neutrino sensitivity above 20 PeV to Earth interacting tau neutrinos for both long-duration transient neutrino sources, such as that for a binary neutron star (BNS) merger [7], and short-duration neutrino transients such as that from short gamma-ray bursts (sGRBs) [8]. These results demonstrate the potential for using the beamed optical Cherenkov light generated by extensive air showers (EAS) from upward-moving τ-lepton decay to observe cosmic neutrinos with energy thresholds in the PeV-decade, even with the inherent optical atmospheric attenuation. This motivated the development of *vSpaceSim*, to provide a comprehensive cosmic neutrino modeling package, which also includes EAS radio generation, to develop space-based and balloon-borne experiments. The initial development has focused on developing a robust Python-based software architecture to both model the optical Cherenkov signal and geomagnetic radio signal from upward-moving EASs sourced from ν_τ's interacting in the Earth. Related simulation development has indicated that the Cherenkov signals from upward-EASs from Earth-interacting ν_μ's dominate for $E_\nu \lesssim 1$ PeV [9]. Given these results and recent ANITA radio detection measurements [10, 11], including a class of events consistent with that from Earth-emerging τ-leptons observed near the Earth's limb, there is rich potential for space-based and sub-orbital cosmic neutrino measurements. The goal of the *vSpaceSim* program is to provide an efficient and practical cosmic neutrino EAS signal generation simulator to the community that provides a standard to gauge the neutrino measurement performance and the effects of modeling systematic errors in the development of sub-orbital and space-based experiments, including transient modeling capability over the entire celestial sky.

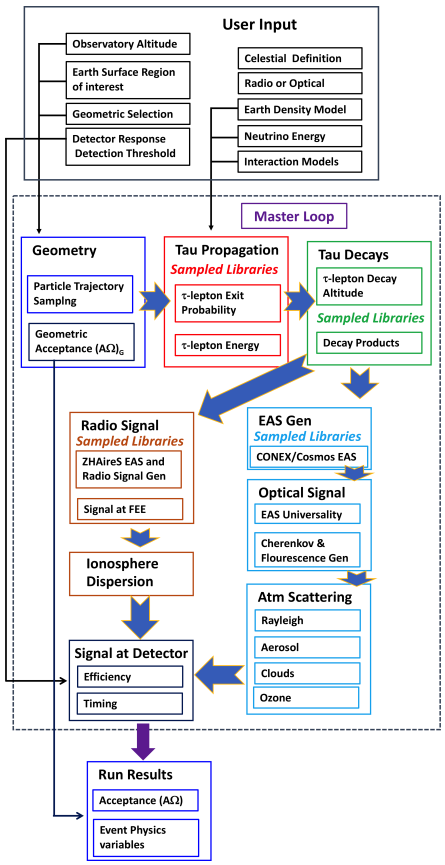

Figure 1: The *vSpaceSim* flowchart detailing the modular functionality of the software package.

2. *ν*SpaceSim Software Framework

νSpaceSim employs a vectorized Python scheduler wraps user input and physics modules that employ a sampled libraries methodology in a manner to include the determination of the event and celestial geometry to facilitate astrophysical source analysis, including transients, in the code. The initial *νSpaceSim* modeling is focused on calculating the neutrino apertures (km^2 sr) and effective areas (km^2) for Earth-interacting tau neutrinos leading to Earth-emergent τ-leptons that decay to generate upward-moving EAS. Each component of the *νSpaceSim* software conforms to the standard interface of a callable Python module. Individual modules are written in Fortran, C, or C++, and wrapped in Python to facilitate data exchange between separate modules. Components are designed to process input arrays of independent event data efficiently in the underlying language, and output to the Python scheduler result arrays of contiguous data, a methodology known as "vectorization." Operating on contiguous data takes advantage of the architecture of modern processors, including multi-core threading, while using the hierarchy of small, on-chip memory caches available on modern CPUs to enable faster memory accesses. By passing references to data arrays these vectorized modules communicate efficiently in Python, while retaining the performance of the underlying high-level language. Intermediate and output values are optionally written to disk in the efficient HDF5 data format, the standard used in *νSpaceSim*. The user supplies configuration parameters for each simulation via an input XML file with defined schema, with automatic detection of invalid settings. The resulting simulator tool is both an easy-to-use command line tool and a well-defined hierarchy of importable high-performance Python modules.

2.1 Simulation & Physics Modules

The *νSpaceSim* user and physics modules, including event and celestial geometry determination, sampling the τ-lepton Earth-emergence probability and energy distributions, generation of the τ-lepton decay products, sampling of EAS profile libraries, generation of the optical Cherenkov and radio EAS signals, propagation of the signals through the atmosphere (including the effects of clouds on the optical Cherenkov signal) and modeling the detector response. A private GitHub repository is used for internal software development, and Repoman is being used for git version control and the seamless assembly of separate GitHub objects into a common toolset. *νSpaceSim* will be hosted on NASA/GSFC High Energy Astrophysics Science Archive Research Center (HEASARC) [12] as well as the support programs `nuPyProp`, detailed in Ref. 13 in these proceedings, and a web-based tool to determine cloud and aerosol atmospheric distributions obtained from the NASA MERRA-2 database [14]. Here we summarize the *νSpaceSim* modules in Fig. 1.

Geometry Module: Each simulation begins with a call to the *νSpaceSim* geometry module that defines the geometry of the region of interest using user defined input. Randomly generated event trajectories throughout this region are sampling the geometrical distributions appropriate for the Earth viewing constraints. The Python scheduler then passes acceptable trajectories to the physics modules in order to generate the EAS and their signals at generation and at the detector to determine the detection probability for each event. Key input geometry parameters include the altitude of the detector and its maximum and minimum viewing angles with respect to the Earth's limb. *νSpaceSim* thus calculates a detector's acceptance for a given input neutrino energy.

τ-lepton P_{Exit} Generation: *vSpaceSim* generates the τ-lepton Earth-exit probabilities and energy spectra using `nuPyProp` [13], a Python-based program will be complete that generates look-up tables for $\nu_\tau \rightarrow \tau$ propagation in the Earth, key inputs to the simulation of upward-going EAS. Look-up tables are also generated for $\nu_\mu \rightarrow \mu$. For incident ν_τ, the propagation through the Earth involves a series of neutrino interactions and τ-lepton decays (regeneration), while for ν_μ, a single $\nu_\mu \rightarrow \mu$ is included. `nuPyProp` has a flexible structure with two neutrino interaction models two lepton electromagnetic energy loss models for their transit through the Earth, and a simplified model of τ-lepton decays to regenerate ν_τ's.

For lepton electromagnetic interactions with in materials, the implementation of the energy loss through either stochastic or continuous energy loss has the potential to impact τ-lepton exit probabilities and energy distributions. The *vSpaceSim* τ-lepton propagation has been developed with stochastic energy loss. The `NuTauSim` code uses continuous energy loss [15], and *vSpaceSim* will have an option to use `NuTauSim` generated libraries. Fig. 2 shows the τ-lepton P_{Exit} distributions as a function of incident tau neutrino energy and Earth-emergence angles [13].

τ-lepton Decay and EAS Development Modeling: In order to model EAS Cherenkov and radio signals from τ-leptons emerging from the Earth, *vSpaceSim* models the τ-lepton decay that generates the EAS and defines the optical Cherenkov and radio signal characteristics. The *vSpaceSim* philosophy is to provide the user with several options for modeling τ-lepton decays: 1) The EAS energy is set to a user-provided constant value times the τ-lepton energy. (The default value is 0.5, consistent with τ-lepton decay simulations performed in recent studies [c.f., 16].) 2) τ-lepton decay events are randomly selected from an HDF5 database of a billion decay events generated from Pythia 8 [17] simulations. 3) τ-lepton decay events are generated using a module that samples τ-lepton decay channels according to their relative branching ratios and the parameters of final state particles from an HDF5 lookup table of energy and momentum distributions constructed from Pythia 8 simulations. The first option has already been implemented in the current version of *vSpaceSim*.

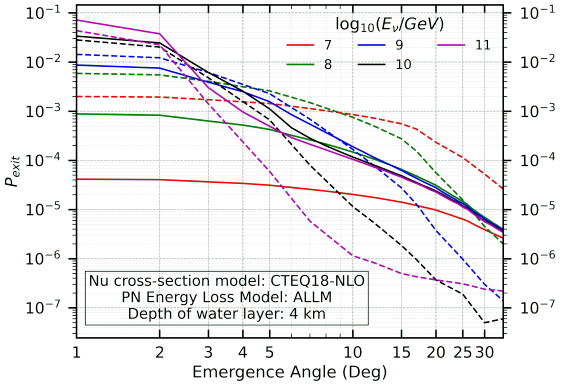

Figure 2: τ-lepton P_{Exit} versus tau neutrino energy and Earth-emergence angles using CT18-NLO neutrino cross sections and ALLM photonuclear τ-lepton energy loss model: $\nu_\tau \rightarrow \tau$ (solid); $\nu_\mu \rightarrow \mu$ (dashed). Ref. 13.

Event and distribution databases have been generated using Pythia, with the implementation of the second and third options are near completion. Functionality will also be provided to allow the user to supply their own event and/or distribution tables. Once the energies of the τ-lepton decay products are determined for a specific decay channel, the resultant EASs are generated based on the location of the τ-lepton decay, where the altitude of the EAS development is a function of the Earth-emergence angle and the energy of the emitted τ-lepton, both provided within the Python scheduler. When viewed from a distance of more than ~10 km, the EAS can be well approximated as a line along which the shower progresses, at first brightening then diminishing, thus a 1-D model of development of the longitudinal EAS profile is sufficient. Fast and efficient 1-D air shower gener-

ators exist, e.g. CONEX [18] in the CORSIKA [19] EAS simulation package. CONEX is used to generate the longitudinal profiles of EASs as a function of altitude, with each profile described by the Gaisser-Hillas 4-parameter function. This is performed as a function of initiating particle and EAS starting altitude. [20]. A specific feature produced by detailed simulations such as CONEX, is a tail in the late EAS stage dominated by muons, whose effect is fit in the Gaisser-Hillas parameters provided by the simulation, although care must be taken since the fit involves a quadratic function of the slant depth (g/cm$^\circ$) for the λ parameter. The Greisen parameterization [21] is included in $\nu SpaceSim$ for comparison studies, and the comparison to the CONEX results is shown in Fig. 3). However, with proper considerations of the modeling of the evolution of the charged-particle content of EASs, composite EAS can be formed using the specific decay products provided in the PYTHIA τ-lepton decay libraries.

Optical Cherenkov Light Generation: The fluorescence and Cherenkov light from an EAS can be predicted using shower universality [22], the concept that all EASs are similar with respect to location a maximum shower development. Using the angular distribution of EAS electrons/positrons and the known atmospheric index-of-refraction, the angular distribution of Cherenkov photons can be tabulated. The shape of the Cherenkov-photon angular distribution is independent of EAS energy, so a table can be pre-computed for efficient use in the simulation. The angular distribution then is just a function of EAS stage and atmospheric index-of-refraction. The Cherenkov universality libraries are currently being integrated into $\nu SpaceSim$, An example of the expected lateral distribution of Cherenkov light density from a 100 PeV shower emerging from sea level at 5° is shown on the right in Figure **??** for a detector in a 525 km orbit, but not including the effects of atmospheric attenuation. The width of the tails of this distribution crucially effect the effective aperture for acceptance of optical Cherenkov events, especially for relatively bright signals from higher energy events. Thus, accurately modeling the optical Cherenkov light profile is critical due to its strong effect on an experiment's geometry factor and neutrino aperture.

Atmospheric Attenuation Modeling: The baseline atmospheric model uses the 1976 Standard US atmosphere to define the pressure and temperature variation as a function of altitude. For the optical Cherenkov modeling, a baseline model of the index of refraction of air as a function of altitude is given by the NIST shop-floor model Ignoring clouds, EAS signals in the UV to optical range have three scattering/attenuating components: Rayleigh scattering, Mie (aerosol) scattering, and ozone absorption. Rayleigh scattering is straightforward to calculate as it is dependent on the slant depth between the point of generation on the EAS and an observation point. While the majority of the air fluorescence yield is between 300 - 400 nm, the observed optical Cherenkov signal can span a much larger wavelength band (200 - 1000 nm), depending on the level of atmospheric attenuation Rayleigh scattering and Mie (aerosol) scattering deplete the shorter wavelength component of the Cherenkov spectrum more strongly. The impact of Mie scattering for the Cherenkov signal is amplified due to the small Earth-emergence angles of the τ-leptons and the fact that their EAS may occur at low altitudes, especially for $E_\tau \lesssim 10^{8.5}$ GeV due to the relatively short τ-lepton decay length at these energies. A model for calculating the wavelength dependence of Mie scattering based on Elterman [23] is used, which also defines a baseline aerosol altitude profile, which are available as look-up tables. The Earth's ozone layer efficiently attenuates signals for $\lambda \lesssim 300nm$ and a baseline ozone model [24] is used.

Optical signals from EAS are affected by clouds, which can scatter and absorb the light. Given

the orbital parameters of a space-instrument or an estimate of the trajectory for a balloon flight, one can infer the cloud cover probability in the field-of-view of the instrument. A robust framework was developed to read out the cloud modelling information constrained by real data provided by NASA's MERRA-2 database [14]. The MERRA-2 data are integrated in *vSpaceSim* with a resolution of 0.625° in longitude and 0.5° in latitude and values available every hour of every day, a monthly average Cloud Top Pressure (CTP) probability distribution can be created for each pixel. Using an atmospheric model of the user's choosing, a corresponding Cloud Top Height (CTH) can be generated, and to facilitate a web interface via HEASARC [12] will provide access.

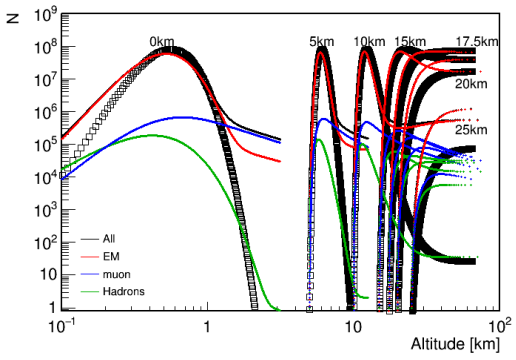

Figure 3: The average longitudinal EAS profiles from the CONEX simulation for 100 PeV pions for 5° Earth-emergence angle as a function of EAS starting altitudes. The various components (solid lines) are compared to the Greissen parameterization (black boxes).

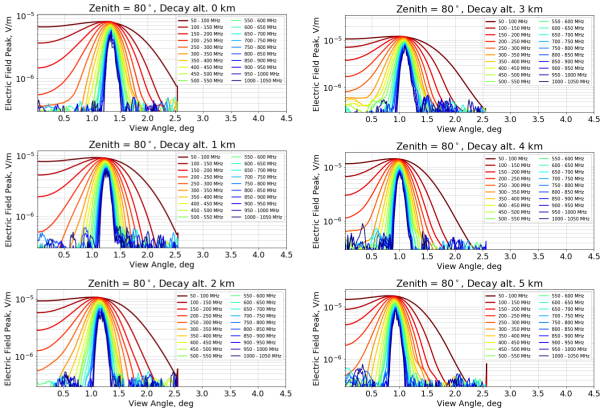

Figure 4: Results from the ZHAireS simulation showing the radio pulse spectra at 525 km altitude as a function of observer view angle of the shower for a zenith angle of 80° τ-lepton decay altitude.

Optical Detector Modeling: The resultant optical Cherenkov spectrum and time distribution after atmospheric attenuation is recorded at the altitude of the detector. These results are then processed assuming an instrument response function, which includes effective area and optics point-spread-function (PSF) as a function of the viewing direction to the Cherenkov light generated by the EAS. A Poisson probability funtion is then applied using a photo-detection-efficiency (PDE) wavelength-dependent function. A separate tool determines the needed photo-electron (PE) threshold needed to minimize the effects of the dark-sky air glow background, see Refs. 2019PhRvD.100f3010R,PhysRevD.102.123013,2021NIMPA.98564614K. The PE threshold is set in the input xml user file.

Geomagnetic Radio Generation: The radio emission from an EAS is due to the combination of several classical radiation mechanisms [25]. The evolving electron and positron distributions in the EAS are deflected by the Earth's magnetic field, resulting in radio emission due to the time-varying transverse currents in the shower. A small atmospheric refractivity is sufficient to produce a Cherenkov-like radiation effect that focuses the radio emission forward along the propagation axis of the EAS. The combination of these effects is referred to as geomagnetic radiation. The EAS also produces an excess negative charge due to the dominance of electrons over positrons, leading to an additional Askaryan-like [26] contribution to the radio emission. The properties this radiation produce a characteristic radio impulse spectrum and polarization that make EAS

events straightforward to recognize. The Cherenkov-like effects produce an impulsive electric field with a spectrum that increases linearly up to 5 MHz, is flat up to ~100 MHz [25], and then falls exponentially at higher frequencies [27]. The radio emission beam is aligned with the EAS propagation axis with a beam width of ~3° at $\nu \approx 50$ MHz, and produces a narrow cone peaking at ~1° from the EAS axis with 0.5° width at 300 MHz. The geomagnetic field deflects the charged particles in the EAS in a plane that is orthogonal to the magnetic field vector and the direction of propagation via the Lorentz force law. Since the Earth's magnetic field is well known [28], and the beam is forward-directed, the impulse shape and polarization provide a signature for the radio measurement of EAS events.

vSpaceSim employs look-up tables of the electric fields generated by τ-lepton decay EAS, dispersion of the radio signal through the ionosphere, and using a simplified model for the trigger of a radio receiver based on electric field thresholds. Simulation results based on ZHAireS [25] were further developed from the study of upward-moving EAS at sub-orbital altitudes [29] to model EAS radio signals at Low-Earth orbits (~500 km altitude). These simulations were employed to produce look-up tables of radio signals as a function of EAS energy, trajectory, and τ-lepton decay altitude to be used in the *vSpaceSim* Python scheduler. 4 shows an example result of the ZHAireS simulations used in the radio EAS library definition for one specific Earth-emergence angle of 10° as a function of τ-lepton decay altitude. In the development of the radio tables, a surprising saturation effect for high-altitude EAS was discovered, which is detailed in Ref. 30 in these proceedings.

2.2 *v*SpaceSim Results: β-version

The current *vSpaceSim* version is constructed with the optical Cherenkov modeling methodology used to predict the neutrino sensitivities for the POEMMA mission [16, 31], e.g. assuming 50% τ-lepton decay energy into the EAS, Greissen EAS parameterization, Hillas Cherenkov light generation parameterization [21, 32], and a static atmosphere using the atmospheric attenuation model in Refs. 16, 31. Fig. 5 shows the modeling results for a POEMMA-like experiment, but with 360^c*irc* azimuth coverage, with a comparison to the results presented in Refs. 16, 31 for the calculation of the diffuse tau neutrino aperture. The results show excellent agreement between the original simulation and the implementation in *vSpaceSim* . It should be noted that each simulation for a given ν_τ energy threw 10^6 events and the processing took less than 20 minutes on a 2017-vintage Mac PowerBook. Fig. 5 shows the result from the initial complete *vSpaceSim* end-to-end chain for the optical Cherenkov modeling demonstrating good agreement with the result in Ref. 16.

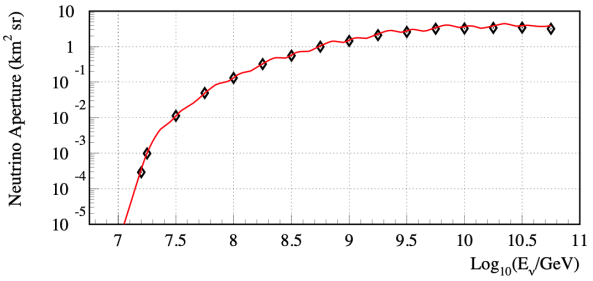

Figure 5: The tau neutrino aperture for an instrument with 2.5 m^2 effective area, < PDE >= 0.2 , and PE threshold to lead to < 0.01 false neutrino events from the dark-sky airglow background per year. The black diamonds are the *vSpaceSim* β results while the red curve is that from the simulation used in Ref. 16.

3. Acknowledgements

This work is supported by NASA grants 80NSSC19K0626 at the University of Maryland, Baltimore County, 80NSSC19K0460 at the Colorado School of Mines, 80NSSC19K0484 at the University of Iowa, and 80NSSC19K0485 at the University of Utah, 80NSSC18K0464 at Lehman College, and under proposal 17-APRA17-0066 at NASA/GSFC and JPL.

References

[1] M. G. Aartsen et al., Advances in Space Research **62**, 2902 (2018), 1701.03731.
[2] M. G. Aartsen et al., Phys. Rev. D **98**, 062003 (2018).
[3] M. G. Aartsen et al., Nature **591**, 220 (2021).
[4] M. G. Aartsen et al., Science **361**, eaat1378 (2018), 1807.08816.
[5] R. Stein and other, Nature Astronomy **5**, 510 (2021), 2005.05340.
[6] A. V. Olinto, J. F. Krizmanic, et al., Journal of Cosmology and Astroparticle Physics **2021**, 007 (2021).
[7] K. Fang and B. D. Metzger, Astrophys. J. **849**, 153 (2017), [Astrophys. J.849,153(2017)], 1707.04263.
[8] S. S. Kimura, K. Murase, P. Mészáros, and K. Kiuchi, APJL **848**, L4 (2017), 1708.07075.
[9] A. L. Cummings, R. Aloisio, and J. F. Krizmanic, Phys. Rev. D **103**, 043017 (2021), 2011.09869.
[10] ANITA Collaboration, P. W. Gorham, et al., Phys. Rev. D **99**, 122001 (2019), 1902.04005.
[11] ANITA Collaboration, P. W. Gorham, et al., arXiv e-prints arXiv:2008.05690 (2020), 2008.05690.
[12] NASA's High Energy Astrophysics Science Archive Research Center (HEASARC).
[13] S. Patel and M. H. Reno, in *37th International Cosmic Ray Conference (these proceedings* (2021).
[14] R. Gelaro, W. McCarty, M. J. Suarez, R. Todling, A. Molod, L. Takacs, C. A. Randles, A. Darmenov, M. G. Bosilovich, R. Reichle, et al., Journal of Climate **30**, 5419 (2017).
[15] J. Alvarez-Muniz et al., Phys. Rev. **D97**, 023021 (2018), 1707.00334.
[16] M. H. Reno, J. F. Krizmanic, and T. M. Venters, Phys. Rev. D **100**, 063010 (2019).
[17] T. Sjöstrand et al., Computer Physics Communications **191**, 159 (2015), 1410.3012.
[18] T. Pierog, M. K. Alekseeva, T. Bergmann, V. Chernatkin, R. Engel, D. Heck, N. N. Kalmykov, J. Moyon, S. Ostapchenko, T. Thouw, et al., Nuclear Physics B Proceedings Supplements **151**, 159 (2006), astro-ph/0411260.
[19] D. Heck, T. Pierog, and J. Knapp.
[20] T. K. Gaisser and A. M. Hillas, in *Proceedings of the 15th ICRC (Plovdiv)* (1977), vol. 8, pp. 353–357.
[21] A. M. Hillas, J. Phys. G: Nucl. Phys. **8**, 1475 (1982).
[22] D. Bergman, in *International Cosmic Ray Conference* (2013).
[23] L. Elterman, Tech. Rep. AFCRL-68-0153, Air Force Cambridge Research Laboratories (1968).
[24] J. F. Krizmanic, in *Proceedings of the 26th ICRC* (1999), vol. 2, pp. 388–391.
[25] J. Alvarez-Muñiz, W. R. Carvalho, and E. Zas, Astroparticle Physics **35**, 325 (2012), 1107.1189.
[26] G. A. Askaryan, JETP **14**, 441 (1962).
[27] J. Alvarez-Muñiz, W. R. Carvalho, Jr., A. Romero-Wolf, M. Tueros, and E. Zas, Phys. Rev. **D86**, 123007 (2012), 1208.0951.
[28] E. Thébault et al., Earth, Planets and Space **67**, 79 (2015), ISSN 1880-5981.
[29] A. Romero-Wolf et al., Phys. Rev. D **99**, 063011 (2019).
[30] A. Romero-Wolf et al., in *37th International Cosmic Ray Conference (these proceedings)* (2021).
[31] T. M. Venters, M. H. Reno, J. F. Krizmanic, L. A. Anchordoqui, C. Guépin, and A. V. Olinto, Phys. Rev. D **102**, 123013 (2020).
[32] A. M. Hillas, J. Phys. G: Nucl. Phys. **8**, 1461 (1982).

+νSpaceSim Collaboration

John Krizmanic[1,2,3] Yosui Akaike[4], Luis Anchordoqui[5], Douglas Bergman[6], Isaac Buckland[6], Austin Cummings[7], Johannes Eser[8], Claire Guépin[9], Simon Mackovjak[10], Angela Olinto[8], Thomas Paul[5], Sameer Patel[11], Alex Reustle[3,12], Andrew Romero-Wolf[13], Mary Hall Reno[11], Fred Sarazin[14], Tonia Venters[3] Lawrence Wiencke[14], Stephanie Wissel[7]

[1]Center for Space Sciences and Technology, University of Maryland, Baltimore County, Baltimore, Maryland 21250 USA, [2]Center for Research and Exploration in Space Science & Technology, [3] NASA/Goddard Space Flight Center, Greenbelt, Maryland 20771 USA, [4]Waseda Institute for Science and Engineering, Waseda University, Shinjuku, Tokyo, Japan, [5]Department of Physics and Astronomy, Lehman College, City University of New York, New York, New York, 10468 USA, [6] Department of Physics and Astronomy, University of Utah, Salt Lake City, Utah 84112 USA, [7] Department of Physics, Pennsylvania State University, State College, Pennsylvania 16801 USA, [8] Department of Astronomy and Astrophysics University of Chicago, Chicago, Illinois 60637 USA, [9] Department of Astronomy, University of Maryland, College Park, College Park, Maryland 20742 USA, [10] Institute of Experimental Physics, Slovak Academy of Sciences, Kosice, Slovakia, [11] Department of Physics and Astronomy, University of Iowa, Iowa City, Iowa 52242 USA, [12] INNOVIM, [13] Jet Propulsion Laboratory, California Institute of Technology, Pasadena, California 91109, USA, [14] Department of Physics, Colorado School of Mines, Golden, Colorado 80401 USA

PoS(ICRC2021)1205